UC Irvine
UC Irvine Previously Published Works

Title

The local marine reservoir effect at Kalba (UAE) between the Neolithic and Bronze Age: An indicator of sea level and climate changes

Permalink

https://escholarship.org/uc/item/3bh7p9fd

Authors

Lindauer, Susanne
Santos, Guaciara M
Steinhof, Axel
et al.

Publication Date

2017-10-01

DOI

10.1016/j.quageo.2017.09.003

Peer reviewed

The local marine reservoir effect at Kalba (UAE) between the Neolithic and Bronze Age: An indicator of sea level and climate changes

CrossMark

Susanne Lindauer [a,b,*], Guaciara M. Santos [c], Axel Steinhof [d], Eisa Yousif [e], Carl Phillips [f], Sabah A. Jasim [e], Hans-Peter Uerpmann [g], Matthias Hinderer [b]

[a] Curt-Engelhorn-Zentrum Archaeometry, Klaus-Tschira-Archaeometry-Centre, C4, 8, 68159 Mannheim, Germany
[b] Institute of Applied Geosciences, Technical University Darmstadt, Schnittspahnstr. 9, 64287 Darmstadt, Germany
[c] Earth System Science, University of California, Irvine, B321 Croul Hall, Irvine, CA 92697-3100, USA
[d] Max-Plack Institute for Biogeochemistry, Hans-Knöll-Str. 10, 07745 Jena, Germany
[e] Directorate of Antiquities, Department of Culture & Information, Sharjah, United Arab Emirates
[f] UMR 7041, ArScAn du CNRS, Maison René Ginouvès de l'Archéologie et de l'Ethnologie, 21 Allée de l'Université, 92023 Nanterre cedex, France
[g] Center for Scientific Archaeology, Eberhard-Karls-University Tübingen, Rümelinstraße 23, 72070 Tübingen, Germany

A R T I C L E   I N F O

A B S T R A C T

We investigate the local marine reservoir effect at Kalba, United Arab Emirates (UAE), between the Neolithic and Bronze Age with respect to possible changes through time and mollusk species diversity. Two distinctive species living in close proximity to the mangrove of Khor Kalba provide insights into ocean circulation patterns in this coastal environment. The species selected are the bivalve *Anadara uropigimelana*, and the gastropod *Terebralia palustris*. They have been an important local food resource for humans since at least the Neolithic. Our results show that for the Neolithic and Bronze Age, the reservoir effects ΔR are quite different for the species selected. For *Anadara* spp. the ΔR decreases from 576 ± 90 to 112 ± 44 years, while for *Terebralia* spp. the reduction ranges from 389 ± 66 to −19 ± 36 years. These results are coeval with other multi-proxies (stalagmite records and sea level changes) for the middle Holocene, and suggest that the main cause of the decreasing reservoir effect is a changing — in this case declining - sea level and an increasingly drier climate.

1. Introduction

In arid environments preservation of organic material is rather insufficient. To build reliable radiocarbon (^{14}C) chronologies all possible materials must be taken into account, including those of fossil shells originating from shallow-water coastal areas and estuaries. However, marine shells tend to be radiocarbon depleted (i.e. ^{14}C-deficient) compared to their atmospheric counterparts, creating offsets that must be accounted for in order to be properly used in chronological models. The reason for the depletion in ^{14}C of marine organisms lies in the fact that oceans can store carbon in the deep sea for up to 1000 years. Upwelling ocean circulation transports old carbon to the surface which is then incorporated by the organisms. The specific offset between coeval terrestrial-shell samples can be expressed as Marine reservoir effect ΔR or just ΔR. The effect is well described in the publications of Dutta (2008) and Southon et al. (2002).

Earlier investigations in the Indian Ocean (including the Arabian Sea) concerning local marine reservoir effects observed in shells were restricted to the pre-bomb period, and to museum collections of shells collected alive mainly during the 19th century or from archaeological excavations (Southon et al., 2002; Dutta, 2008; Zazzo et al., 2012). Here then a mean ΔR was determined by using all available shells, independent of species or possible temporal variability, apart from one recent publication (Zazzo et al., 2016). For sites where all organic materials are relatively scarce this approach might be unavoidable, and for shell species sharing similar habitats and food resources, it might be even acceptable (Ascough et al., 2005).

We draw your attention to a location on the coast of the Gulf of Oman, Kalba (Fig. 1), which shows signs of human occupation since Neolithic times, as well as signs of an intact mangrove forest for about the same timespan. During archaeological excavations shell

---

* Corresponding author. Curt-Engelhorn-Zentrum Archaeometry, Klaus-Tschira-Archaeometry-Centre, C4, 8, 68159 Mannheim, Germany.
E-mail address: Susanne.lindauer@cez-archaeometrie.de (S. Lindauer).
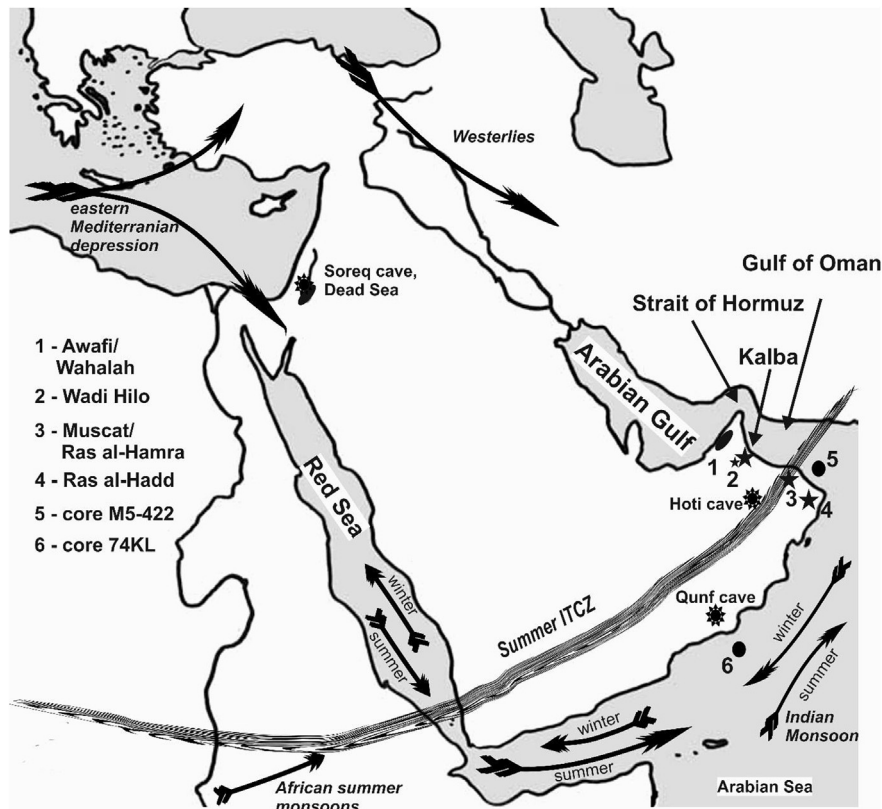
Fig. 1. Map with Kalba, UAE, in the context of the paleoclimate proxies (Soreq cave, Dead Sea, Hoti cave, Qunf cave, Awafi lake, Wahalah lake, sediment cores) that are discussed in the text. The arrows represent the dominant wind directions including seasonality that influence our area of interest.

middens and settlements with shell layers were found.

This allowed us to address local reservoir effects in the following three ways:

1) We investigated its dependence on shell species by analyzing, the marine bivalve *Anadara uropigimelana* and the mangrove gastropod *Terebralia palustris.* We also determined the local ΔR change over time of both species by comparing Neolithic and Bronze Age sites in Kalba.
2) These results are then discussed regarding the earlier investigations on the reservoir effect calculated for neighboring areas.
3) The long-term changes on regional climate and environmental conditions. If we see a change in ΔR over time it needs to be discussed in comparison of climate proxies of neighboring areas to be able to judge whether or not these changes are caused by climatic effects or only food resources of the shells for example. Food is an important factor of carbon storage in the shell. Hence e.g. mangroves leaves as a food resource result in a lower reservoir effect than algae. For our shells this is already discussed in Lindauer et al. (2016).

An earlier publication (Lindauer et al., 2016) explained how shells in Kalba reflect the environment they live in, and whether the species *Anadara* and *Terebralia* spp. were suitable candidates to study ΔR in this region. Preliminary results for the shell midden KK1 during the Neolithic period showed a significant age offset compared to the contemporaneous terrestrial material, but the lack of statistical significance due to the low number of specimens of *Anadara* spp. called for further analysis. Moreover, the complexity of the Arabian Peninsula ecoregion, with its coastal mangroves and

intricate ancient history, demanded the sampling of a younger archaeological site (e.g. K4) to help with comparisons and discussion.

With our research we intend to go one step further and take all possible ecosystem drivers (e.g. upwelling strength, sea level changes and climate, shell species and their dietary habits) into account to better understand any ΔR variability in this location. For proper ΔR interpretations and to obtain quantitative uncertainties when deriving reservoir effects from isolated locations in a specific region, shell species and ecosystem attributes are as important as the local oceanic and climatic conditions. Once we understand how those combined effects can affect ΔR, we may be able to successfully describe its temporal variation in the past.

1.1. Regional setting and archaeology

Kalba is an enclave in the Emirate Sharjah located on the Gulf of Oman, United Arab Emirates (UAE). Being part of the Arabian Sea (see Fig. 1), the Gulf of Oman is also known as the Oman Sea, but for consistency with international publications we will use Gulf of Oman here. At this site, the Hajar Mountains rise steeply from the coastline. Old shell middens dating back to the Neolithic spread along the beach as shown in Fig. 3. South of Kalba there is a lagoon with occasional freshwater from rainfall and a mangrove forest known as Khor Kalba with an extensive sabkha surrounding the mangroves today. Here we studied the Neolithic shell midden Khor Kalba site 1 (KK1) and the Bronze Age settlement Kalba 4 (K4) further north near the modern town Kalba. In order to maintain consistency across works, we use the names of the sites as introduced by Phillips and Mosseri-Marlio (2002).

The oldest shell midden KK1 is located near the foot of a hill

between the Hajar Mountains and the sabkha (supratidal salt flat). Apart from shells, bifacial stone tools were also found, indicating that the site was visited during the 5th millennium BC (Phillips and Mosseri-Marlio, 2002). Other sites, such as KK2-13 are relatively younger (around 3000 yrs BP for shells, see Phillips and Mosseri-Marlio (2002)) especially towards the beach line (Fig. 3). The major archaeological finds in this region, including the distinct settlements and tombs, date back to the Bronze and Iron Age period. The mound referred to as K4 has revealed several superimposed building phases as described by Phillips and Mosseri-Marlio (2002). The earliest period is associated with a circular tower structure around which, during the middle of the second millennium BC, a large mud-brick tower was built. Further construction continued during the Iron Age, including a large wall around the settlement. It is possible that the settlement was abandoned during the first millennium BC. Nevertheless, it is certain that the mangroves at Khor Kalba were already there during the Neolithic period, and most probably served as an important source of food and wood to the settlers and/or travelers (Phillips and Mosseri-Marlio, 2002).

1.2. Chronological aspects and radiocarbon

Several methods exist today to help establish the chronology of an archaeological site or a paleoenvironment. Apart from stratigraphic and archaeological context, such as artifactual evidence for human occupation(s) (such as flint stones and pottery fragments), sediments can be dated using optically stimulated luminescence (OSL) or sedimentological methods. Certainly plenty of marine shells can be found at archaeological sites along the coast, or even inland. At the coastline, where the molluscs were harvested by humans, the remains can be found deposited as shell middens. Further inland, they appear as grave goods or undefined archaeological finds, as for example in Wadi al-Hilo around 20 km southwest of Kalba (Kutterer et al., 2012; Uerpmann et al., under review). As already mentioned these marine shells appear to be older in ^{14}C ages compared to terrestrial materials, due to the upwelling of old carbon in this marine habitat (see Fig. 2). Therefore ΔR can vary geographically due to different upwelling intensity, changing ocean circulation patterns, sea level change or freshwater inflow to name only some important controlling factors. Hence we speculate that the marine reservoir effect in Kalba may not necessarily be constant over time. Moreover, shells apparent ages can vary due to species dietary habits (Ascough et al., 2005; Culleton et al., 2006). Different food-resources and habitats can lead to differences in the marine reservoir effect. Therefore, species special traits such as food resources and shifts over their habitat conditions, must be properly investigated.

The marine reservoir effect in the Gulf of Oman has been investigated previously by others, e.g (Southon et al., 2002; Dutta, 2008; Zazzo et al., 2012, 2016). The publications by Southon and Dutta together with their co-workers used data on shells from museum collections that were collected alive before 1945. They determined ΔR values of e.g. 163 yrs for Qatar in the Arabian Gulf and 285 years for Muscat. Zazzo et al. (2012, 2016) found data slightly lower than the Muscat data, as will be discussed in detail in comparison with our data.

Throughout this publication uncalibrated radiocarbon ages will be cited as ^{14}C yrs BP, whereas calibrated ages will be mentioned as cal yrs BP or in case of several thousand years as ka cal BP.

1.3. Holocene climate variability

Paleoclimate investigations concerning the Holocene in South-East Arabia have been undertaken using a variety of materials: lake and dune deposits (Parker et al., 2006a,b; Enzel et al., 2015; Parker et al., 2016), marine sediment records (Staubwasser et al., 2002; Leuschner and Sirocko, 2003), speleothems (Fleitmann et al., 2007; Fleitmann and Matter, 2009; Van Rampelbergh et al., 2013) to name but a few. The highest paleoclimatic resolution in this region is provided by the speleothem records of Hoti cave in North Oman, and Qunf Cave (South Oman). Sedimentary records from the Dead Sea further north (Migowski et al., 2006; Weninger et al., 2009), and other lake records from the Arabia also provide interesting information regarding the climatic system for this area. The marine sediment cores are less intense in signal, but nevertheless provide information about the ocean at the times of interest. There are many more paleoclimate investigations that are not mentioned but point in the same direction. We decided to compare our data with key, representative sites.

A common finding among these archives is the fact that South Arabia appeared to have been way wetter during the early Holocene (i.e. between 10 ka and 6 ka ago) than nowadays (Parker et al., 2006a,b). Controversies exist regarding the exact ending of this wet period. The controversy appears to be related to specific locations, as reviewed in Van Rampelbergh et al. (2013). While sedimentary records of the Arabian Sea and the speleothem records of South Oman suggest a gradual decrease in precipitation since approximately 8 ka years ago, records from Northern Oman and the United Arab Emirates (e.g. the speleothems in Hoti cave and the sedimentary records of the Rub al-Khali) indicate that the end of the wet period came rather abrupt around 6 ka. Note that among the sites studied so far, those that suggest a sudden change in wetness are nowadays outside the Intertropical Convergence Zone (ITCZ) as indicated in Fig. 1. The northernmost position of the ITCZ during summer shifted to the south of the UAE and North Oman around 6 ka ago, disconnecting these areas from monsoonal rains. This leaves winter Westerly rainfall as the main source of precipitation (Parker et al., 2006a,b), and winds coming from the West (see Fig. 1). Soreq Cave and the Dead Sea are also influenced by these Westerly winds, which is one of the reasons why we want to compare our data also to these locations further north. The wind directions plotted in Fig. 1 show the complex patterns with seasonal change that also are reflected in the ocean circulation shown in Fig. 2.

1.4. Ocean circulation and geology

Near Kalba the seafloor is rather flat and the Gulf of Oman narrows towards the Strait of Hormuz. The water current here is complex, as it reverses direction seasonally (Fig. 2) and probably depends on the direction of the ocean currents that are described for different seasons. The water at Kalba is not only influenced by the waters of the Arabian Sea, but also by the Arabian Gulf (Johns et al., 2000; Dalongeville and Sanlaville, 2005). During winter the upwelled deep waters from the Arabian Sea flow near the Kalba coastline site and over the Straits of Hormuz into the Arabian Gulf (red arrows in Fig. 2). In the summertime the outflow from the Arabian Gulf passes by Kalba hereby affecting the water mixing in the mangrove estuary (blue arrows in Fig. 2). This is in accordance with the wind directions in Fig. 1. The Arabian Gulf itself is very flat and has a high evaporation rate which increases temperature and salinity. Apart from the carbonaceous rocks and sediments the strong evaporation enhances the development of minerals including gypsum (Purser, 1973).

The ocean floor in the Gulf of Oman becomes significantly steeper near Muscat and Ras al-Hadd (see Fig. 1 for locations, Fig. 2 for bathymetry). Between Kalba and Ras al-Hamra, near Muscat, the seafloor drops from several hundred to over 2000 m. Here the denser water sinks to the bottom and away from the coast. South of Muscat and also Ras al-Hadd the waters show a stronger exchange as the Arabian Sea is wider open.
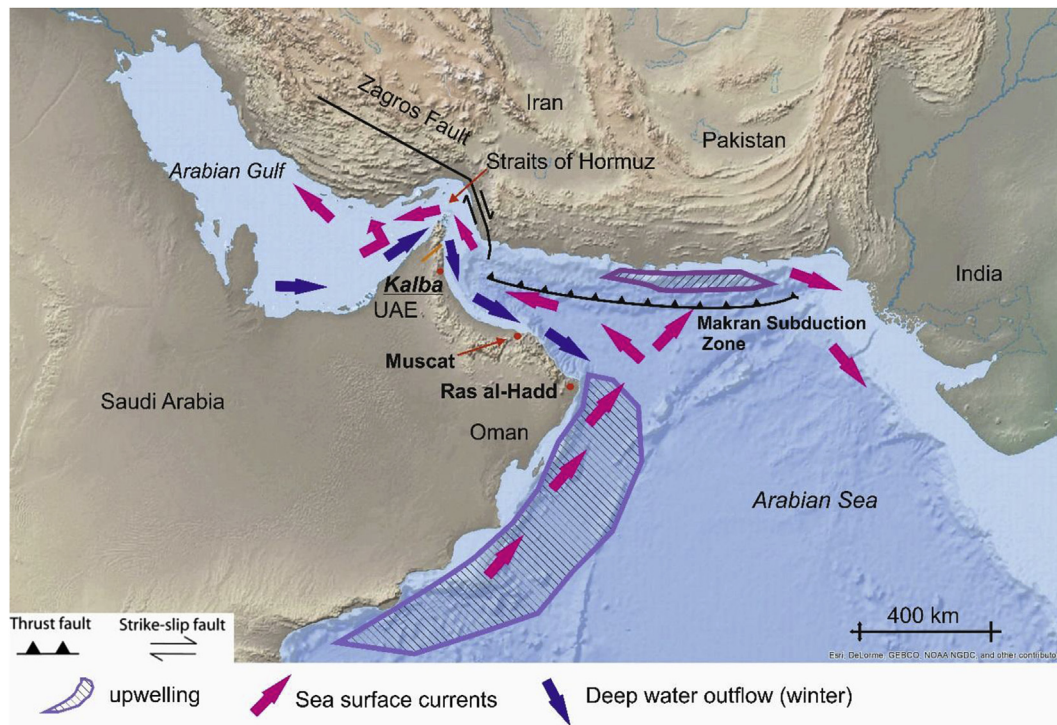
Fig. 2. Map showing bathymetric and terrestrial heights with modern seasonal ocean circulation patterns and upwelling water from Arabian Sea. The Dibba zone is marked as an orange line. Map modified after (Schneider et al., 2016) with information on upwelling from (Staubwasser et al., 2002) and seasonal flow directions from (Dalongeville and Sanlaville, 2005). (For interpretation of the references to colour in this figure legend, the reader is referred to the web version of this article.)

Sea level change during the Holocene has varied with a possible high stand occurring around 6 ka cal BP when the water could have been 2–3 m higher than today (Bernier et al., 1995; Lambeck, 1996; Lambeck et al., 2011). This sea level height might be relative because geological evidence shows that the Arabian Plate near the Straits of Hormuz is moving north (Hoffmann et al., 2013).

Along the Straits of Hormuz the Arabian plate is subducting. The Arabian Peninsula is characterized by Ophiolite, the old Tethys Ocean floor, with local differences in mineral composition, and overlying Carbonates. Along the coastal margins fracture zones and subduction zones can be found. Strong wave events are documented in sediments found near ancient settlements and point to very active tectonics (Hoffmann et al., 2015).

2. Materials and methods

2.1. Site description, sample collection and rationality

Shell and ash samples from the shell midden KK1 at Khor Kalba (see Fig. 3) were taken 2013. Details of the shells midden can be found in (Phillips and Mosseri-Marlio, 2002). The shell midden although quite large in extent is only about 50 cm high with respect to the shells. There is no layered structure apart from an extensive lens of ashy sediment at the bottom. Only through radiocarbon dating was it was possible to recognize two distinct periods of accumulation. The preliminary ^{14}C investigations and respective ΔR calculation regarding these samples were published (Lindauer et al., 2016). During 2015 this shell midden was re-sampled, aiming to collect a more representative population of *Anadara* spp. shells from the lowermost KK1 layer. This layer also contains lots of ashy sediment. Only three more *Anadara* specimens were found at the outermost edge of the ashy sediment. We also collected a second sample from the ash at the edge to verify the previous ^{14}C

dating result, because the relative sampling positions was not identical (see Fig. 3). If the results for the two ash samples are different it is possible to calculate two reservoir effects for KK1 and see whether they overlap or whether they are different within errors.

The shell midden KK1 shows two distinct time ranges for the shells and the ashes. There are approximately 7000 ^{14}C yrs BP at the bottom and 6300 ^{14}C yrs BP (shell ages) immediately above until the surface of the midden (~50 cm). Occasionally, ashy sediment age determinations can pose a problem, because this type of carbonaceous material can contain carbon from multiple sources, e.g. charcoal and/or carbon inclusions in minerals (Braadbaart et al., 2012). Therefore, measurements of δ^{13}C were used to examine the possible origin of the carbon in the ashy sediment.

In order to verify possible changes in ΔR over time, we sampled a second site in Kalba, K4 (Fig. 3). This site was once a settlement inhabited during the Bronze and Iron Age, and was excavated during the 1990s (Phillips and Mosseri-Marlio, 2002). We found two layers of shells, ash, and charcoal fragments next to an Iron Age mudbrick wall. The charcoal fragments of the lower layer were in association with burnt date stones. Distinct charcoal or charred date stones are ideal terrestrial reference material for determining ΔR. As mentioned earlier, ash samples are often difficult to interpret. The lower layer (named "MBZ1" hereafter) is approximately 30 cm thick, and besides the presence of charcoal and burnt date stones, it also contains fragments and unbroken specimens of *Anadara* spp. and *Terebralia* spp. This layer is overlain by another layer extremely rich in shells, referred to as "MBZ2". This layer is around 30–40 cm thick, and is slightly inclined towards the mud brick wall (Fig. 3). MBZ2 layer hardly contained any ash, however we managed to find half of a bivalve of *Anadara* spp. with a charcoal fragment embedded in it. It was not immediately clear whether the two layers MBZ1 and MBZ2 are significantly different in age even
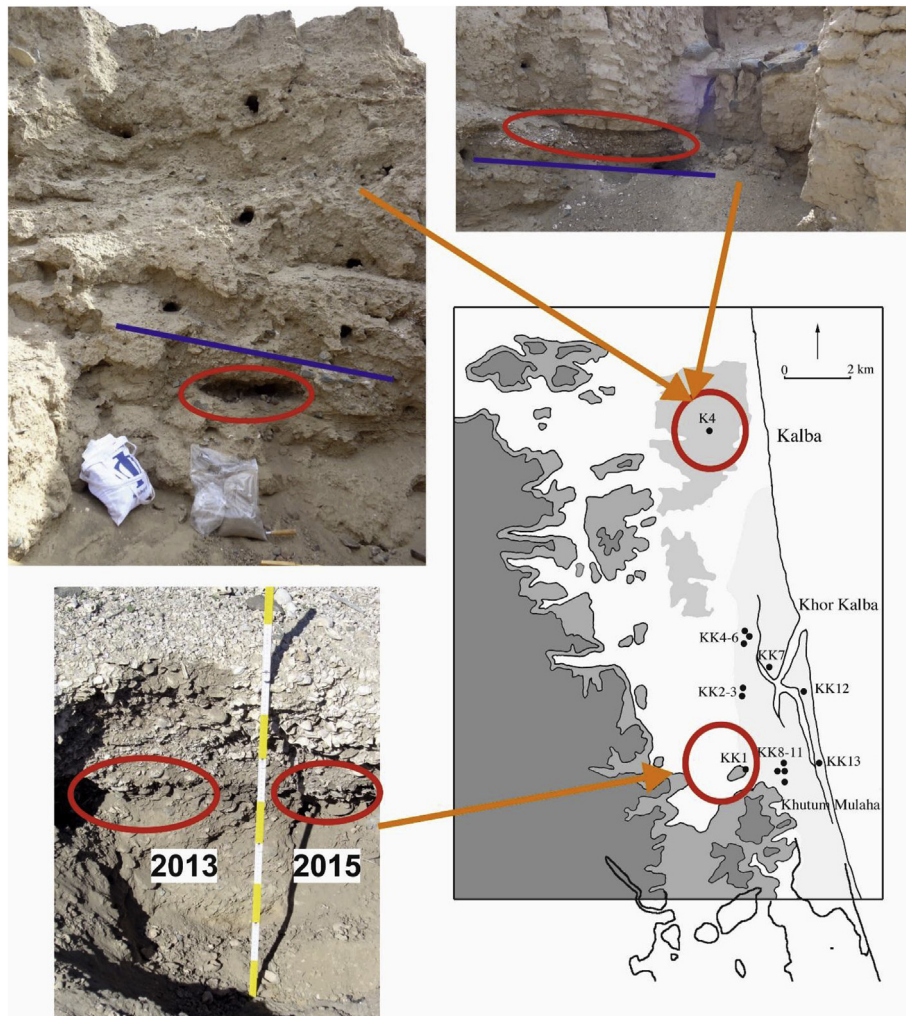
Fig. 3. The sites at Kalba studied here (red circles) include the settlement K4 and the Neolithic shell midden KK1 located at the edge of the mangrove and sabkha area. The upper left photo shows sampling of the lower layer MBZ1 (below blue line). The upper right photo depicts the shell-rich layer MBZ2 (above blue line) slightly tilted to the right at K4 site. The vertical structure visible to the right is part of the mud brick wall mentioned in the text. The bottom photo was taken in 2013 and shows part of the shell midden KK1 where the samples had been taken (red circles). The map with the locations at the right was modified from (Phillips and Mosseri-Marlio, 2002), photos S. Lindauer. (For interpretation of the references to colour in this figure legend, the reader is referred to the web version of this article.)

though they are clearly separated. Through ^{14}C measurements we obtained a clear picture of their time sequences.

To constrain the possible age ranges within the layers, we sampled and ^{14}C dated several specimens of both *Anadara* spp. and *Terebralia* spp. per site and layer (Table 1).

2.2. Sample pretreatment for isotopic analysis

The ^{14}C measurements were conducted in multiple laboratories, hence sample processing and subsequent analysis differed slightly among facilities. The facilities involved are the German laboratories of Curt-Engelhorn-Zentrum Archaeometry Mannheim (CEZA Mannheim ^{14}C lab; sample code *MAMS*), Max-Planck-Institute for Biogeochemistry Jena (MPI-BGC Jena; sample code *P*), and the USA facility Keck Carbon Cycle AMS (KCCAMS; sample code *UCIAMS*). Some of the major differences on sample processing and analysis are described below.

Shells were sampled at the ventricular margin to determine a date as close as possible to the time of death, being aware that due to the ontogenetic age trend in shells it is possible to sample a time span of more than one year. For analysis performed at CEZA

Mannheim ^{14}C lab and MPI-BGC Jena, the outer surface contamination was removed by etching with 1% HCl and washing with Milli-Q water three times. The carbonate samples at CEZA were hydrolyzed using 85% phosphoric acid in an autosampler system by Ionplus in combination with the Age III graphitization system also by Ionplus (Wacker et al., 2013; Lindauer et al., 2016). Graphite samples were then measured by the MICADAS AMS system at the ^{14}C lab of the Klaus-Tschira-Archaeometrie-Zentrum, Mannheim (Kromer et al., 2013). In the Jena lab aragonite from shells was extracted using a headspace extraction at a special inlet to the graphitization system and measured using the 3 MV Tandetron accelerator (HVEE, Amersfoort, Netherlands) at the MPI-BGC Jena (Steinhof et al., 2004). At KCCAMS carbonate fragments were physically inspected under microscope, 30% leached and also hydrolyzed using 96% phosphoric acid in disposable blood vials (Santos et al., 2004; Santos and Xu, 2016). The cryogenically clean CO_2 released was transferred to reaction volume for graphitization following established protocols (Santos et al., 2007), and then measured at a modified NEC 0.5 MV 1.5SDH-2 compact AMS system (Beverly et al., 2010).

Charcoal and charred date stone samples received the same

Table 1
List of sites in Kalba with number of samples per shell specimen and organic matter collected.

Period	Site	Layer	Year of collection	Material	No of samples
Bronze Age	K4	MBZ2	2015	*Anadara* spp.	5
				Terebralia spp.	4
				charcoal	1
		MBZ1		*Anadara* spp.	5
				Terebralia spp.	5
				charcoal	1
				charred date stone	1
Neolithic	KK1		2013	*Anadara* spp.	2
				Terebralia spp.	5
				ash	1
			2015	*Anadara* spp.	7
				Terebralia spp.	3
				ash	1

pretreatment before being measured at CEZA Mannheim or MPI-BGC Jena. They were given an ABA treatment consisting of 4% HCl followed by 0.4% NaOH and a final HCl step. Each chemical steps had a duration of 60 min. While the HCl steps were done at elevated temperature (60 °C), the NaOH step was carried out at room temperature. In between and after all steps the chemicals were removed with Milli-Q water. Ashy sediments were pretreated the same way as charcoal samples with the difference that the first acid step was done at room temperature as long as a reaction could be seen with renewal of acid in between, until no further reaction could be detected (Lindauer et al., 2016). Terrestrial samples were then combusted using an elemental analyzer (Vario Micro, Elementar) and graphitized using a self-built graphitizer system that uses liquid nitrogen to fill the reactors (Lindauer and Kromer, 2013). At the MPI-BGC Jena the prepared ash and charcoal samples were combusted using an elemental analyzer (NC2500, Carlo Erba, Milano, Italy) before the CO_2 gas was collected by the UGCS (Universal Gas Collection System) line including a cryogenic trap and 20 ports for graphitization reactors (Steinhof et al., 2004). At KCCAMS we also processed and measured ashy and charcoal samples using an ABA procedure with the main difference being the chemical strength applied (e.g. 1 N HCl and 1 N NaOH, with both digestions applied at 60 °C), as it is described in (Santos and Ormsby, 2013). Chemically clean organics were subjected to sealed tube combustion to produce CO_2, and thus graphitized as per carbonate samples, before ^{14}C-AMS measurements at the spectrometer (Santos and Xu, 2016).

Isotopic analyses of δ^{13}C were performed from ash and ash/charcoal samples at the Earth System Science Research Center, Institute of Geosciences, University Mainz for MAMS-samples (Lindauer et al., 2016) and at the Earth System Science, University of California, Irvine, for the KCCAMS samples. Ash is normally composed of a complex matrix with microscopic sizes of charcoal fractions and carbonaceous minerals (Braadbaart et al., 2012), and therefore can present difficulties in determining their chronology. Thus, the stable isotope ratio mass spectrometer (IRMS) measurements performed here have the intent to draw information concerning the sample carbon source(s) of those materials. While some AMS instruments do provide online-δ^{13}C values, those are also a product of instrument fractionation and therefore are used solely to correct the ^{14}C data for these effects (Santos et al., 2007; Lindauer and Kromer, 2013). At KCCAMS CO_2 aliquots from pre-treated ash and ash/charcoal were recovered after combustion and measured by using a continuous flow stable isotope ratio mass spectrometer (Delta-Plus CFIRMS) interfaced with a Gasbench II (for CO_2 input). Stable isotope results are reported as values in ‰ relative to the Vienna Pee Dee Belemnite (vPDB). Total organic carbon has also

been determined by using a Fision NA 1500NC elemental Analyzer from Finegan DeltaPlus IRMS. At the Institute for Geosciences in Mainz the δ^{13}C of the charcoal sample (MAMS 22875) was measured using a Flash2000 Elementar Analyzer (Thermo) with a Finnigan MAT 253 stable isotope ratio mass spectrometer. Results are reported in the same way as at KKCAMS.

Radiocarbon data are being reported as uncalibrated ages (^{14}C yrs BP) following recommended conventions for the reporting of ^{14}C (Stuiver and Polach, 1977). As mentioned before calibrated ages are reported as cal BP. To calibrate the conventional ^{14}C ages we used Oxcal 4.2 with the Intcal13 dataset (Bronk Ramsey and Lee, 2013; Reimer et al., 2013). The reservoir effects were modelled for each site separately (KK1 and K4). We used a phase model in Oxcal with undetermined reservoir effect ΔR, as presented in (Zazzo et al., 2016).

3. Results and discussion

3.1. Radiocarbon measurements and reservoir effects ΔR

The complete isotopic results are presented in Table 2. The results for the two mollusk species *Anadara* spp. and *Terebralia* spp. show a species-specific ΔR, as suggested by Lindauer et al. (2016) with *Anadara* spp. showing tentatively higher reservoir effects ΔR than *Terebralia* spp. The δ^{13}C measurements of both parts of the KK1 ash layer point to a wooden material (C3 plant) as major carbon component. Therefore, we conclude that their ^{14}C results are suitable to be used as terrestrial analogue for reservoir effect ΔR calculations. Moreover, the younger ^{14}C age range of part of the shell fragments in the KK1 shell midden suggests a second occupation period during later times which is relevant for archaeologists. Hence, we decided to calculate two reservoir effects to account for each time-frame/layer and shell species during the Neolithic.

The reservoir effect ΔR for *Anadara* spp. declines from 576 ± 90 yrs to 200 ± 30 yrs during the Neolithic. For *Terebralia* spp. the change in ΔR shows a reduction from 389 ± 66 yrs to 172 ± 99 yrs for the same period, e.g. between 7.0 and 6.5 ka cal BP. This corresponds to a change in reservoir effect of more than 350 yrs for *Anadara* spp. and nearly 200 yrs for *Terebralia* spp. within just 600 yrs (calibrated ages of terrestrial material in Table 3).

The archaeological site Kalba K4 yielded two time periods as well (3530 and 3420 ^{14}C yrs BP), both matching the Middle Bronze Age. Here we were able to measure distinct charcoal pieces (J 13304), charred date stone (J 13305), and another charcoal sample (UCIAMS171125 & −171126). As the MBZ1 and MBZ2 layers can be clearly distinguished (Table 2 and Fig. 3), calculating a reservoir

Table 2
Individual radiocarbon data on shells and contemporary terrestrial material (ash, charcoal, charred date stone) are shown, including duplicates. The ΔR values represent 2σ probability distributions. Only δ^{13}C data from IRMS measurements is given. The order of magnitude of the uncertainty of these results is of 0.1‰ based on measurements of multiple standards (e.g. ATP- Atropine, USGS 24-graphite). Samples published in (Lindauer et al., 2016) can be recognized by their MAMS code as they had been renamed for consistency.

Site/Layer	Labcode	Sample ID	Material	^{14}C age (yrs BP)	δ^{13}C (‰)	%C	ΔR (yrs)
KK1	*MAMS 22875*	*KK1 2013 ash*	*Ash*	*6117 ± 26*	*−25.2*	*5.3*	
	MAMS 29217	KK1 2013 Ana2	A. uropigimelana	7073 ± 30			Anadara spp. 576 ± 90
	MAMS 22878	KK1 2103 Ana1	A. uropigimelana	7058 ± 27			
	MAMS 22876	KK1 2013 Ter1	T. palustris	6911 ± 28			Terebralia spp.
	MAMS 22877	KK1 2013 Ter2	T. palustris	6924 ± 27			389 ± 66
	UCIAMS171097	KK1 2015 Ter1	T. palustris	6870 ± 20	−4.2		
	UCIAMS171098	KK1 2015 Ter2	T. palustris	6855 ± 25	−4.5		
	UCIAMS171099	KK1 2015 Ter3	T. palustris	6850 ± 20	−4.5		
KK1	*UCIAMS173933*	*KK1 2015 ash*	*Ash*	*5755 ± 20*	*−20.8*	*5.0*	
	UCIAMS173934	*KK1 2015 ash*	*Ash (duplicate)*	*5690 ± 20*	*−20.6*	*5.0*	
	MAMS 22867	KK1 2013 Ana3	A. uropigimelana	6295 ± 26			Anadara spp. 200 ± 30
	MAMS 22880	KK1 2013 Ana4	A. uropigimelana	6273 ± 27			
	MAMS 22883	KK1 2013 Ana5	A. uropigimelana	6310 ± 26			
	MAMS 22885	KK1 2013 Ana6	A. uropigimelana	6272 ± 27			
	UCIAMS171094	KK1 2015 Ana1	A. uropigimelana	6305 ± 15	−2.4		
	UCIAMS171095	KK1 2015 Ana2	A. uropigimelana	6300 ± 20	−1.4		
	UCIAMS171096	KK1 2015 Ana3	A. uropigimelana	6295 ± 20	−0.9		
	P 14279	KK1 2015 Ter1	T. palustris	6386 ± 28			Terebralia spp.
	MAMS 22882	KK1 2013 Ter3	T. palustris	6257 ± 26			172 ± 99
	MAMS 22884	KK1 2013 Ter4	T. palustris	6262 ± 26			
K4/MBZ1	*P13304*	*K4 MBZ1 char*	*Charcoal*	*3531 ± 40*			
	P 13305	*K4 MBZ1 DS*	*Date stone*	*3537 ± 35*			
	P 13306	K4 MBZ1 Ana1	A. uropigimelana	3954 ± 54			Anadara spp. 105 ± 50
	P 13307	K4 MBZ1 Ana2	A. uropigimelana	3891 ± 35			
	P 13308	K4 MBZ1 Ana3	A. uropigimelana	3989 ± 38			
	P 13309	K4 MBZ1 Ana4	A. uropigimelana	3983 ± 40			
	P 13310	K4 MBZ1 Ana5	A. uropigimelana	3976 ± 50			
	P 13311	K4 MBZ1 Ter1	T. palustris	3958 ± 42			Terebralia spp.
	P 13312	K4 MBZ1 Ter2	T. palustris	4224 ± 43			−26 ± 46
	P 13313	K4 MBZ1 Ter3	T. palustris	3764 ± 41			
	P 13314	K4 MBZ1 Ter	T. palustris	3732 ± 45			
	P 13315	K4 MBZ1 Ter5	T. palustris	3845 ± 45			
K4/MBZ2	*UCIAMS171125*	*K4 MBZ2 char*	*Charcoal*	*3425 ± 15*	*−24.0*	*61.0*	
	UCIAMS171126	*K4 MBZ2 char*	*Charcoal (duplicate)*	*3420 ± 15*	*−23.0*		
	UCIAMS171084	K4 MBZ2 Ana1	A. uropigimelana	3825 ± 15	−2.1		Anadara spp. 112 ± 44
	UCIAMS171085	K4 MBZ2 Ana2	A. uropigimelana	3835 ± 15	−1.2		
	UCIAMS171086	K4 MBZ2 Ana3	A. uropigimelana	3830 ± 15	−1.7		
	UCIAMS171087	K4 MBZ2 Ana4	A. uropigimelana	3880 ± 15	−1.6		
	UCIAMS171088	K4 MBZ2 Ana5	A. uropigimelana	3945 ± 15	−1.4		
	UCIAMS171089	K4 MBZ2 Ter1	T. palustris	3690 ± 15	−3.0		Terebralia spp.
	UCIAMS171090	K4 MBZ2 Ter2	T. palustris	3690 ± 15	−4.8		−19 ± 36
	UCIAMS171091	K4 MBZ2 Ter3	T. palustris	3715 ± 20	−3.4		
	UCIAMS171092	K4 MBZ2 Ter4	T. palustris	3790 ± 20	−3.8		

Table 3
Calibrated results of terrestrial samples from Kalba. Calibration was done using Oxcal 4.2 with the IntCal13 dataset.

Labcode	Sample ID	Material	Radiocarbon ages			
			Uncalibrated	Calibrated		
			yrs BP	cal BP (1σ)	cal BP (2σ)	mean cal BP
MAMS 22875	KK1 2013 ash	Ash	6117 ± 26	7146–6946	7156–6906	7013 ± 69
UCIAMS173933	KK1 2015 ash	Ash	5755 ± 20	6601–6499	6634–6493	6557 ± 41
UCIAMS173934	KK1 2015 ash	Ash (dup.)	5690 ± 20	6491–6445	6508–6408	6465 ± 26
P 13304	K4 MBZ1 char	Charcoal	3531 ± 40	3828–3714	3854–3644	3762 ± 51
P 13305	K4 MBZ1 DS	Date stone	3537 ± 35	3835–3721	3868–3694	3775 ± 48
UCIAMS171125	K4 MBZ2 char	Charcoal	3425 ± 15	3695–3641	3719–3632	3671 ± 28
UCIAMS171126	K4 MBZ2 char	Charcoal (dup.)	3420 ± 15	3692–3640	3705–3614	3667 ± 25

effect for this period was much more straightforward.

The Neolithic shell midden KK1 and the sampled Middle Bronze Age archaeological site K4 are apart by nearly 3000 yrs. During this period the reservoir effect ΔR was further reduced to 105 ± 50 yrs (MBZ1) and 112 ± 44 yrs (MBZ2) for *Anadara* spp., and −26 ± 46 yrs (MBZ1) and −19 ± 36 yrs (MBZ2) for *Terebralia* spp., respectively (Table 2). We found unexpected high shell

species-dependency in ΔR.

3.2. Comparison of the ΔR results with other published data

Zazzo et al. (2016) determined ΔR values based on *A. antiquata* collected at Ras al-Hamra (at the RH6 prehistorical site) located on the east coast of Oman, near Muscat (Figs. 1, 2). Assuming that shell

members of the same genus share similar food resources and habitats, we compare our ΔR determinations obtained with the marine species of *A. uropigimelana* with those derived from *A. antiquata* determined in Zazzo et al. (2016). For these comparisons we use our data drawn from the shell midden KK1, e.g. the terrestrial layers collected in 2013 and 2015, which is more or less contemporary to the data at Ras al-Hamra and dated to (see Table 3) 7013 ± 69 cal BP (MAMS 22875) and 6557 ± 41 cal BP (UCIAMS173933) as well as its duplicate measurement of 6465 ± 26 cal BP (UCIAMS173934) reported in Table 3. For *A. uropigimelana* we determined a ΔR of 576 ± 90 (±2σ) and 200 ± 30 (±2σ) yrs, respectively. Zazzo et al. (2016) calculated a ΔR of 202 ± 96 (±1σ) yrs for the oldest layer (subunit SU 185, 7077 ± 49 cal BP). For the younger layer (subunit SU 117, 6675 ± 31 cal BP) the ΔR value calculated by Zazzo et al. (2016) is 144 ± 25 (±1σ) yrs. It should be noted that Zazzo et al. (2016) then used the mean ΔR of all layers they had found. For *T. palustris* a direct comparison cannot be done, because no species specific ΔR for this species was determined by Zazzo or anyone else.

While our ΔR determination overlaps within errors with Zazzo et al. (2016) for the KK1 late period, e.g. for the younger layer, the offset between the older layers is significantly different. The difference in ΔR cannot be attributed to underestimation in uncertainties, as we already report our data with ±2σ errors instead of just ±1σ. Problems with the ^{14}C age determinations from ash samples cannot be evoked either, as our δ^{13}C values point to charred wood as the dominant carbon source in the ash sample. Furthermore, chemical extractions applied were robust and gave consistent results among duplicates (Tables 2 and 3). Assuming that the species-dependent variations in ΔR have been somewhat normalized when comparing results obtained with similar shell species, the distinctive ΔR variability presented here must be due to differences in climatic and oceanic conditions between Ras al-Hamra and Kalba sites at around 7000 cal BP (6100 [4]C yrs BP).

When we take a look at the ocean currents near Kalba and Ras al-Hamra (see 1.4 and Fig. 2) we see that both locations are influenced by different ocean circulation patterns. A steep continental margin closer to the shore should favor a more intense upwelling effect near surface at Ras al-Hamra. Thus, at Ras al-Hamra site one may expect higher ΔR determinations at all times. It is possible that the outflow of the Arabian Gulf carries an increased amount of old carbon due to a higher salinity of the Arabian Gulf as an effect of higher temperature and hence higher evaporation rates. The higher salinity leads to an increased dissolution of limestone and carbon from coral reefs and carbonate sediments and hence an enrichment with old carbon. For the Arabian Gulf it was found that high salinity and temperature together with the extreme aridity have led to an extensive development of evaporate minerals like gypsum (Purser, 1973) as already mentioned. In addition limestone from the subduction zone around the Straits of Hormuz might be dissolved to some extent when the water flows out. This increases the density of the water body (Purser, 1973). This effect might have been stronger during the early Holocene when the sea level at around 6 ka BP was between higher than today and dropped again afterwards (Bernier et al., 1995; Lambeck, 1996). As around 7 ka BP the water level was still rising, more water would flow in and out of the Arabian Gulf. If this current carries high amounts of old carbon this may explain the higher ΔR value along the coast of Kalba over the flat part of the ocean floor. The effect of the outflow at the coast near Ras al-Hamra during the same period of time might be reduced due to the drop in depth of the seafloor and therefore sinking of the denser water. These considerations account for the difference between the two locations, but do not explain the change in ΔR over time.

3.3. Sea level and climate change reflected in a change of ΔR over time

The temporal change in reservoir effect at Kalba from the Neolithic to Bronze Age is significant, and most importantly very high. From this point, a question arises: Why is there a change in the order of several hundred years? A possible reason for such a dramatic offset must be a strong change in environmental conditions. From the shells ^{14}C results alone it remains unclear whether this change happened abruptly, or whether it happened gradually between the Neolithic and Bronze Age periods. Because a change in reservoir effect reflects a change in environmental conditions we need to take a closer look at the environmental or climate proxies investigated by some colleagues.

To properly evaluate this issue, we cross checked our results with those from other works on paleoclimate records in adjacent regions as can be seen in Fig. 1. In Fig. 4 we also highlight the ^{14}C ages of the terrestrial samples associated to our ΔR determinations of the shell midden KK1 and K4 sites in comparison to the data of the other proxies discussed below.

When comparing our data with stalagmite records, those of Hoti Cave are the nearest records. Others stalagmite records that give important information about the periods of interest are those of Qunf Cave (around 600 km south of Hoti), and, further North, Soreq Cave in Israel, southwest of Jerusalem. Regarding stalagmite records, a shift in δ^{18}O to more positive values is interpreted as a reduction in precipitation and hence a shift to a more arid climate (Preston et al., 2015), whereas changes in δ^{13}C reflect changes in vegetation type where an enrichment of δ^{13}C points to an increase in C4 plants to the soil CO_2 (Bar-Matthews and Ayalon, 2004).

Hoti Cave does not show a continuous record throughout the entire Holocene and shows a hiatus between 2.5 and 5.2 ka BP (Fleitmann et al., 2007). Drier periods were recorded for example from 7.5 to 7.2 ka cal BP and from 6.5 to 6.3 ka cal BP, and were less distinct from 5.9 to 5.3 ka BP. This shift in δ^{18}O is interpreted as a southward retreat of the ITCZ (Intertropical convergence zone) and the monsoon rain, followed by a replacement from the southern to a northern moisture source as well as a change in the seasonality of precipitation from summer to winter precipitation (Fleitmann et al., 2007). This coincides with our change in reservoir effect at the shell midden site and its continued influence until at least the duration of the Kalba K4 settlement, as can be seen in Fig. 4.

Qunf Cave however, further south of Kalba, still appeared to be under the influence of the ITCZ after 6.3 ka cal BP. Its δ^{18}O signature gradually decreased about 2‰ between 9 ka and 3 ka cal BP. For Qunf Cave climate conditions were different than for Hoti and hence also for Kalba as the monsoon influenced this cave throughout the Holocene bringing enough rain to support it with drip water for the stalagmite growth and therefore Qunf cave can only give a rough estimate to the environmental conditions influencing the northern region, but shows stronger changes parallel to our shell midden data.

Soreq Cave, although being quite some distance further north of Kalba, shows significant features of its δ^{18}O and especially its δ^{13}C signatures. Between 8.5 and 7.0 ka cal BP the δ^{13}C data seems anomalously high whereas the δ^{18}O only shows a gradual increase. Apart from the strong δ^{13}C event around 8.2 ka cal BP, equivalent to the global cooling event, there are two major changes observed in the data. One is a short pulse in δ^{18}O around 5.2 ka cal BP accompanied by a decrease in δ^{13}C. The second, is an increase in δ^{18}O and δ^{13}C during a period of several hundred years between 4.6 and 4.0 ka cal BP which is interpreted as an increase in C4 vegetation by Bar-Matthews and Ayalon (2004). Anomalously high δ^{13}C values are here interpreted as increased atmospheric CO_2 signal (Bar-Matthews and Ayalon, 2004). The second high δ^{13}C peak around
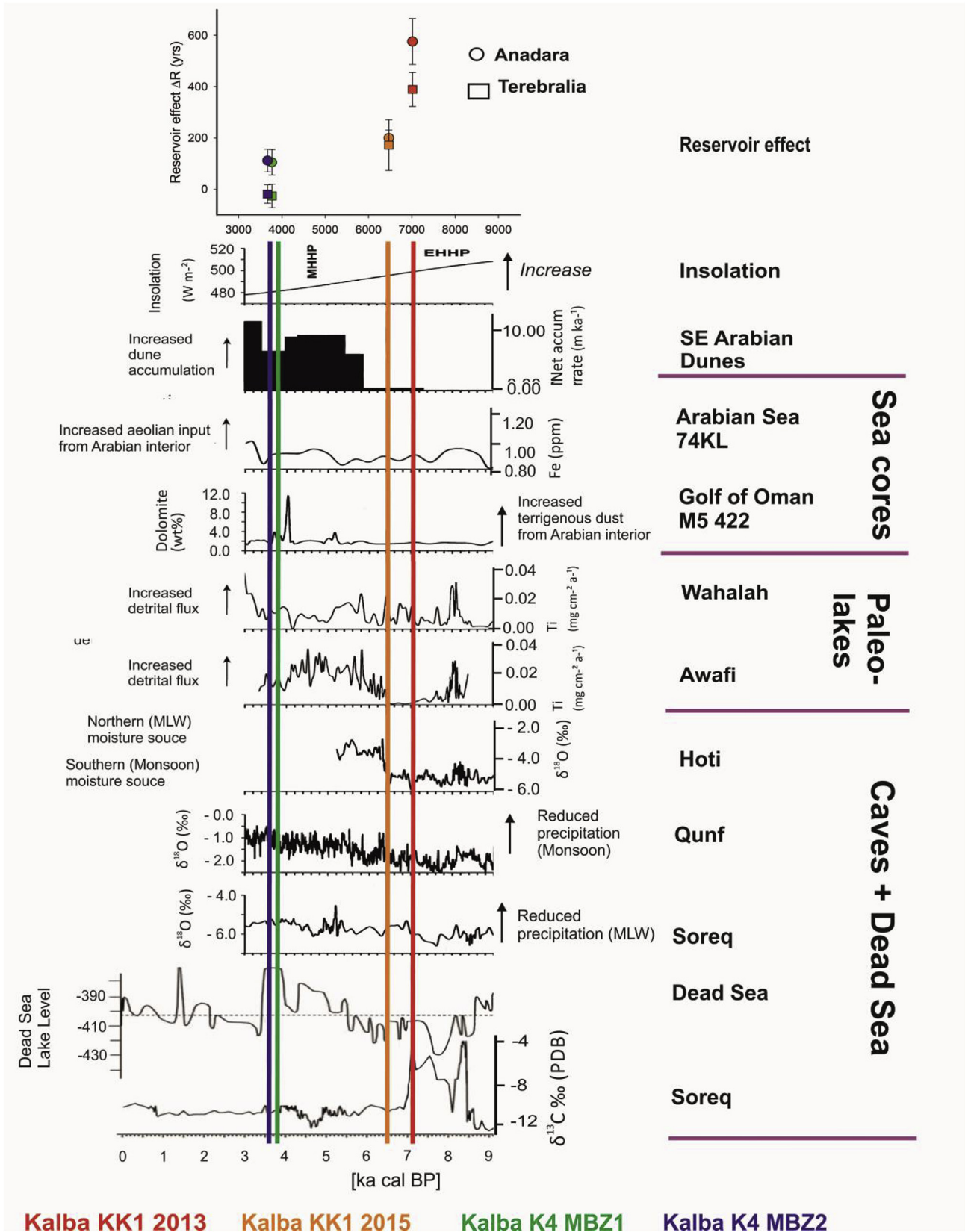
Fig. 4. Comparison of climate proxies, here stalagmites of Oman (Hoti Cave, Qunf Cave) and the Dead Sea lake level, plus Soreq cave in Israel as well as paleolakes in the UAE and sediment cores from the Arabian Sea with calculated reservoir effects. Combined and modified from (Parker et al., 2016) and (Weninger et al., 2009). The periods represented by our data are also shown as colored solid lines and labeled accordingly. Additionally the species specific reservoir effects are plotted on top for comparison.

7 ka BP coincides with our oldest shell midden data whereas the younger shell midden data lies on the plateau following this peak. The $\delta^{18}O$ data is rather unspecific at Soreq during these periods which indicates rather constant water sources (precipitation), maybe due to the Westerlies.

The Dead Sea lake level record seems to corroborate the data from Soreq Cave nearby with stronger features as in the stalagmite records. It seems that the high $\delta^{13}C$ values of Soreq Cave here are contemporary with a drop in water level of the Dead Sea. We have a slow water level rise starting around 6–7 ka cal BP and a final significant rise in lake level just around our K4 MBZ data until about 3500 ka cal BP (Fig. 4), followed by a drastic drop in lake level at the Dead Sea. This supports our finds that our changes in reservoir effect are local but may be linked to changing climates on a larger scale.

The increasing aridity visualized in the hiatus of Hoti can also be seen in the drying out of paleolake sites such as Awafi and Wahalah in the UAE (Fig. 1) as well as the correlated dune development of the Rub al-Khali. Awafi lake shows a reduced detrital sediment input in the period between 7.6 and 6.4 ka cal BP, which is less pronounced in Wahalah lake further southwest (Parker et al., 2016). But both show a significant increase in detrital flux after this time reflected in an increase in the Titanium signal. Here Wahalah lake shows an earlier Titanium and detrital flux signal around 5.9 to 5.2 ka cal BP than Awafi which shows a slow increase between 6.0 and 5.4 ka cal BP followed by a sudden increase until 5.0 ka cal BP (Parker et al., 2016). Both lakes show only minor differences which can be attributed to local effects, but are consistent in the overall pattern, reflecting a change in precipitation as a consequence of a disconnection from the southerly summer rainfall and an increase in sedimentation due to the following increased aridity of the area. This is well in accordance with the interpretation from the stalagmite records and marks the beginning of a landscape reconfiguration (Parker et al., 2016). The deposition of Aeolian sand in Awafi around 4 ka cal BP marks the period of total desiccation. Changes around 4 ka cal BP can be found in several of the paleoclimate records throughout the Arabian Peninsula (Arz et al., 2006; Parker et al., 2016), but also in other regions influenced by the monsoon (Staubwasser et al., 2003; Parker et al., 2016). The periods mentioned above (5.9 ka, 4.3–3.9ka) are amongst the periods correlated with rapid climate change and characterized by reduced temperature, increased aridity, major changes in atmospheric circulation and monsoon activity as identified by several scientists (Mayewski et al., 2004; Parker et al., 2016). These climatic effects and the increase in aridity can also be seen in the marine records that have been analyzed by several authors and might be mirrored in a decrease of local marine reservoir effect ΔR.

The marine records as investigated by (Sirocko et al., 1993; Staubwasser et al., 2002) show increased Fe (iron) values at times of greater Aeolian input. The signal is less distinct, e.g. in core 74 KL Arabian Sea, or in core M5 422 from the Gulf of Oman, and times of increased input can be clearly distinguished and correspond to times of changes in the lake records as well as the stalagmite data (Parker et al., 2016). As the Arabian Sea sediment cores show less distinct features we can only use the overall patterns that can be distinguished, but they also support our finds of a reduction in reservoir effect due to a change in ocean water. The increased input from aeolian sediment reflects a drier environment (more sediment available due to increased aridity) and possibly also a reduced sea level, especially in the Arabian Gulf, which might be partially due to a lack of freshwater input.

At first sight, the younger ash data from the shell midden KK1 (5755 ± 20 yrs BP; UCIAMS173933) for which we derived a ΔR (*Anadara* spp) of 200 ± 30 (±2σ) years and 172 ± 99 for *Terebralia* spp. seems to fit perfectly with the $\delta^{18}O$ drop in Hoti Cave. The

larger ΔR of 576 ± 90 (±2σ) and 389 ± 66 yrs for *Anadara* spp. and *Terebralia* spp. respectively at 6117 ± 26 yrs BP (MAMS 22875) seems to coincide with a drop in $\delta^{13}C$ at Soreq cave in Jerusalem, Israel, pointing to a wet period contemporaneous with a higher sea level at the Arabian Gulf as we had discussed in section 3.2. This seems to be a rather wide spread than just a local phenomenon.

Local effects also contribute to the way the environmental signal is stored in the proxies of interest. Coastal morphology not only is influenced by marine events, but also by the way sediments, marine as well as aeolian or fluvial, are accumulated in estuarine basins (Al-Farraj, 2005). Al-Farraj (2005) explains the development of sabkhas and estuarine environments in the light of coastal events, sea level change, and terrestrial sediment transport culminating in supratidal salty, dry sabkha, where once mangrove forest was found. This must also be kept in mind for interpretation of the development of the lagoon in Kalba, which also includes a large sabkha up to the shell midden KK1 that lies around 2 m higher than the sea level today. Mangrove habitats over time have been investigated by (Berger et al., 2013) for the coast of Oman. The authors here describe several phases of mangrove development in Oman during the Holocene with respect to sea level and human settlements. During a phase between 5500 and 4800 cal BC (around 6.1 ka ^{14}C yrs BP), which is comparable to phase one at the shell midden KK1, they describe a sea level similar to today This also marks a phase of reduced sea level rise after deglaciation.

The next phase, 4800-4400 cal BC (around 5.8 ka ^{14}C yrs BP) is described as optimum for mangrove development around the complete Arabian Sea documented in the amount of shells found in the archaeological sites pointing to extensive exploitation and interpreted as correlated to a higher sea level along the coasts of Oman, followed by a phase of fluctuations in sea level between 4400 and 3900 cal BC, around 5.5 ka ^{14}C yrs BP (Berger et al., 2013). This phase points to a decrease of spread of mangroves due to a decrease in sea level recorded in the Arabian Gulf and the Arabian Sea accompanied by an abrupt climate change recorded in the Hoti Cave stalagmites. Besides the reduction in terrestrial freshwater input due to reduced precipitation would have an important effect on this ecosystem. Towards the end of this period the sea level rises again, but only for a short period of time, followed by a drop in sea level and a further decrease of mangroves. The next period between 3800 and 3500 cal BC (around 5.4 ka ^{14}C yrs BP) is described as a second optimum for mangrove development (Berger et al., 2013) with a high sea level in the Arabian Gulf and the northern Gulf of Oman, although less extensive than the previous one. The next phase, 3500-3000 cal BC (ca. 5.2 ka ^{14}C yrs BP), is again described by a lack of mangrove data pointing to a decrease in mangroves and sea level as well as to an increase in aridity. Hence Berger et al. (2013) interpret their data as evidence of past lagoon and mangrove extension during maximum sea level rise and high fluvial activity during the early to mid-Holocene.

The sea level itself is not only dependent on climatic conditions but also on tectonic events such as subduction. Along the Straits of Hormuz we find the Makran Subduction zone which marks the line where the Arabian plate subducts under the Eurasian plate. North of the Dibba zone the peninsula is subducting whereas south of it the Hajar mountains are rising (Hoffmann et al., 2013, 2015). This might lead to erroneous interpretations about sea levels along the coasts of the Gulf of Oman and the Arabian Gulf. For example storm or tsunami events flood the areas of settlements and do not indicate a change in sea level, but can be linked to tsunamis, as found at Ras al-Hadd, south of Muscat (Hoffmann et al., 2015). Here a flooding event took place at around 4450 ± 200 cal BP, most probably due to a tsunami caused by an earthquake along the Makran Subduction Zone. The upwelling of old ^{14}C-depleted carbon in the Arabian Sea is only of minor influence at Kalba as it mainly takes place along the

southern coast of Oman or along the coast of India and Iran. Kalba is basically seasonally influenced by the outflow of Arabian Gulf deep waters (see Fig. 2). as well as from inflow from the Arabian Sea. This leads to a stronger dependence on effects of Arabian Gulf waters and their carbonate contents as discussed in section 3.2. A reduced water body in the Arabian Gulf or an increase of seafloor height (probably caused by subduction of the mountainous regions of the Musandam peninsula) reduces the amount of water flowing out through the Straits of Hormuz as well as the inflow from the Gulf of Oman. A reduction of outflow probably results in less dissolved old carbon flowing past the beaches of Kalba and reducing the reservoir effect further during the MBZ compared to the Neolithic period. A reduction of Arabian Gulf water coincides also with increasing aridity and hence reduced freshwater input from wadis after rainfall. Depending on the Geology the freshwater input can carry depleted ^{14}C waters, hence this resource needs further investigation and will therefore not be included in the discussion so far.

All the climatic information as well as tectonics and local effects lead us to the interpretation that the reduction of the ΔR over time is a reflection of the change in climate including oceanic conditions, overlapped by a species specific difference in ΔR due to food resources and habitat, as suggested by (Lindauer et al., 2016).

4. Conclusions

Lindauer et al. (2016) had already shown that shell species under investigation are influenced by dietary habits as well as environmental conditions, which can impact local ΔR determinations. Here, we go a step further and correlate local ΔR determinations to paleoproxy data, allowing us to better interpret our change in reservoir effect as a reflection of the climate changes with a reduction of in ΔR due to decreasing sea level and increasing sedimentation rate in the lagoon close to Kalba. The two opposing factors would affect the mangrove and eventually its local environment, as described by Al-Farraj (2005). In this comprehensive research we are able to extend the species specific dependency of the reservoir effect also to younger timescales. Although the difference decreases between Neolithic and Bronze Age it remains significant which can be explained by the influences of habitat and food resource. Especially Anadara spp. drops dramatically in ΔR which could reflect the decrease of old carbon in the ocean water. Terebralia spp. on the other hand is strongly influenced by atmospheric carbon due to its feeding on mangrove leaf litter, whereas Anadara spp. is a filter feeder strongly dependent on marine carbon sources.

At Kalba, paired terrestrial/shell ^{14}C data of bivalve Anadara uropigimelana and gastropod Terebralia palustris show species-specific local reservoir effects with consistently higher values derived from Anadara uropigimelana. In addition, we could show that the reservoir effect from both species decreases significantly between Neolithic and Middle Bronze Age. Once our Neolithic ΔR determinations were compared with those further south in Oman, we observed significant differences. Our ΔR values are at least 100 years higher, which can be explained by local ocean circulation patterns and lagoon shoreline development.

Regarding other paleoclimate proxies in the vicinity of the studied area, our data fits well with changes observed in stalagmite records and paleolakes as well as sediment cores from the Arabian Sea. While for the Neolithic period ΔR assessment yield us values of 576 ± 90 years for Anadara spp and 389 ± 66 years for Terebralia spp., respectively, a decrease to 112 ± 44 and -19 ± 36 years were observed from the same species during the Bronze Age. The discontinuity of our data from 7 ka cal BP to 3 ka cal BP can be regarded as a result of all the climate events that took place during this period, and which are reflected in the data of paleoproxies

discussed here. Nevertheless, it appears that those same climatic and sea level changes are mirrored in the reservoir effect changes we observed in our ^{14}C shells over time. Species specific differences remain significant over time although with a decreasing tendency probably due to stronger changes of carbon content in food resources and habitat for Anadara spp. than for Terebralia spp.

The mangrove of Khor Kalba shows exceptionally well how the marine and the terrestrial influences on a estuarine system overlap and take action. We see the results in the reservoir effects of the different shell species, reflecting different pathways of influence through food resource and habitat and including minor, hence local, as well as major climatic influences to describe the situation over a certain period of time.

References

Al-Farraj, A., 2005. An evolutionary model for sabkha development on the north coast of the UAE. J. Arid Environ. 63, 740—755.

Arz, H.W., Lamy, F., Pätzold, J., 2006. A pronounced dry event recorded around 4.2 ka in brine sediments from the northern Red Sea. Quat. Res. 66 (3), 432—441.

Ascough, P.L., Cook, G.T., Dugmore, A.J., Scott, E.M., Freeman, S.T., 2005. Influence of mollusk species on marine ΔR determinations. Radiocarbon 47 (3), 433—440.

Bar-Matthews, M., Ayalon, A., 2004. Speleothems as Palaeoclimate Indicators, a Case Study from Soreq Cave Located in the Eastern Mediterranean Region, Israel. Past Climate Variability through Europe and Africa. Springer, pp. 363—391.

Berger, J.F., Charpentier, V., Crassard, R., Martin, C., Davtian, G., López-Sáez, J.A., 2013. The dynamics of mangrove ecosystems, changes in sea level and the strategies of Neolithic settlements along the coast of Oman (6000-3000 cal. BC). J. Archaeol. Sci. 40, 3087—3104.

Bernier, P., Dalongeville, R., Dupuis, B., de Medwecki, V., 1995. Holocene shoreline variations in the Persian Gulf: example of the Umm al-Qowayn lagoon (UAE). Quat. Int. 29—30, 95—103.

Beverly, R.K., Beaumont, W., Tauz, D., Ormsby, K.M., Von Reden, K.F., Santos, G.M., Southon, J.R., 2010. The Keck carbon Cycle AMS laboratory, University of California, Irvine: status report. Radiocarbon 52 (2), 301—309.

Braadbaart, F., Poole, I., Huisman, H.D.J., van Os, B., 2012. Fuel, Fire and heat: an experimental approach to highlight the potential of studying ash and char remains from archaeological contexts. J. Archaeol. Sci. 39 (4), 836—847.

Bronk Ramsey, C., Lee, S., 2013. Recent and Planned Developments of the Program OxCal.

Culleton, B.J., Kennett, D.J., Ingram, B.L., Erlandson, J.M., Southon, J.R., 2006. Intrashell radiocarbon variability in marine mollusks. Radiocarbon 48 (3), 387—400.

Dalongeville, R., Sanlaville, P., 2005. L'évolution des espaces littoraux du golfe Persique et du golfe d'Oman depuis la phase finale de la transgression postglaciaire. Paléorient 31 (1), 9—26.

Dutta, K., 2008. Marine ^{14}C reservoir age and suess effect in the Indian Ocean. J. Earth Sci. India I (III), 175—188.

Enzel, Y., Kushnir, Y., Quade, J., 2015. The middle Holocene climatic records from Arabia: reassessing lacustrine environments, shift of ITCZ in Arabian Sea, and impacts of the southwest Indian and African monsoons. Glob. Planet. Change 129, 69—91.

Fleitmann, D., Burns, S.J., Mangini, A., Mudelsee, M., Kramers, J., Villa, I., Neff, U., Al-Subbary, A.A., Buettner, A., Hippler, D., Matter, A., 2007. Holocene ITCZ and Indian monsoon dynamics recorded in stalagmites from Oman and Yemen (Socotra). Quat. Sci. Rev. 26 (1—2), 170—188.

Fleitmann, D., Matter, A., 2009. The speleothem record of climate variability in Southern Arabia. Comptes Rendus Geosci. 341 (8—9), 633—642.

Hoffmann, G., Grützner, C., Reicherter, K., Preusser, F., 2015. Geo-archaeological evidence for a Holocene extreme flooding event within the Arabian sea (Ras al Hadd, Oman). Quat. Sci. Rev. 113, 123—133.

Hoffmann, G., Rupprechter, M., Mayrhofer, C., 2013. Review of the long-term coastal evolution of North Oman — subsidence versus uplift [Review der langfristigen Küstenentwicklung Nordomans — Senkung und Hebung]. Z. Dtsch. Ges. für Geowiss. 164 (2), 237—252.

Johns, W.E., Jacobs, G.A., Kindle, J.C., Murray, S.P., Carron, M., 2000. Arabian Marginal Seas and Gulfs. Technical Report 2000-01. University of Miami RSMAS, p. 60.

Kromer, B., Lindauer, S., Synal, H.-A., Wacker, L., 2013. MAMS - a new AMS facility at the Curt-Engelhorn-centre for Achaeometry, Mannheim, Germany. Nucl.

Instrum. Methods Phys. Res. Sect. B Beam Interact. Mater. Atoms 294 (0), 11–13.

Kutterer, A.U., Doppler, S., Uerpmann, M., Uerpmann, H.-P., 2012. Neolithic cremation in south-east Arabia: archaeological and anthropological observations at FAY- NE10 in the Emirate of Sharjah (UAE). Arab. Archaeol. Epigr. 23, 125–144. Wiley-Blackwell.

Lambeck, K., 1996. Shoreline reconstructions for the Persian Gulf since the last glacial maximum. Earth Planet. Sci. Lett. 142 (1–2), 43–57.

Lambeck, K., Purcell, A., Flemming, N.C., Vita-Finzi, C., Alsharekh, A.M., Bailey, G.N., 2011. Sea level and shoreline reconstructions for the Red Sea: isostatic and tectonic considerations and implications for hominin migration out of Africa. Quat. Sci. Rev. 30 (25–26), 3542–3574.

Leuschner, D.C., Sirocko, F., 2003. Orbital insolation forcing of the Indian Monsoon - a motor for global climate changes? Palaeogeogr. Palaeoclimatol. Palaeoecol. 197 (1–2), 83–95.

Lindauer, S., Kromer, B., 2013. Carbonate sample preparation for ^{14}C dating using an elemental analyzer. Radiocarbon 55 (2–3), 364–372.

Lindauer, S., Marali, S., Schöne, B.R., Uerpmann, H.-P., Kromer, B., Hinderer, M., 2016. Investigating the local reservoir age and stable isotopes of shells from southeast Arabia. Radiocarbon 59 (2), 355–372.

Mayewski, P.A., Rohling, E.E., Curt Stager, J., Karlén, W., Maasch, K.A., David Meeker, L., Meyerson, E.A., Gasse, F., van Kreveld, S., Holmgren, K., Lee-Thorp, J., Rosqvist, G., Rack, F., Staubwasser, M., Schneider, R.R., Steig, E.J., 2004. Holocene climate variability. Quat. Res. 62 (3), 243–255.

Migowski, C., Stein, M., Prasad, S., Negendank, J.F.W., Agnon, A., 2006. Holocene climate variability and cultural evolution in the near east from the Dead sea sedimentary record. Quat. Res. 66 (3), 421–431.

Parker, A., Davies, C., Wilkinson, T., 2006a. The early to mid-Holocene moist period in Arabia: some recent evidence from lacustrine sequences in eastern and south-western Arabia. Proc. Sem. Arab. Stud. 36, 243–255.

Parker, A.G., Goudie, A.S., Stokes, S., White, K., Hodson, M.J., Manning, M., Kennet, D., 2006b. A record of Holocene climate change from lake geochemical analyses in southeastern Arabia. Quat. Res. 66, 465–476.

Parker, A.G., Preston, G.W., Parton, A., Walkington, H., Jardine, P.E., Leng, M.J., Hodson, M.J., 2016. Low-latitude Holocene hydroclimate derived from lake sediment flux and geochemistry. J. Quat. Sci. 31 (4), 286–299.

Phillips, C.S., Mosseri-Marlio, C.E., 2002. Sustaining change: the emerging picture of the neolithic to iron age subsistence economy at Kalba, Sharjah emirate, UAE. In: Fifth International Symposium on the Archaeozoology of Southwestern Asia and Adjacent Areas. ARC-Publicaties Groningen, Amman, Jordan.

Preston, G.W., Thomas, D.S.G., Goudie, A.S., Atkinson, O.A.C., Leng, M.J., Hodson, M.J., Walkington, H., Charpentier, V., Méry, S., Borgi, F., Parker, A.G., 2015. A multi-proxy analysis of the Holocene humid phase from the United Arab Emirates and its implications for southeast Arabia's Neolithic populations. Quat. Int. 382, 277–292.

Purser, B.H., 1973. In: Purser, B.H. (Ed.), The Persian Gulf : Holocene Carbonate Sedimentation and Diagenesis in a Shallow Epicontinental Sea. Springer-Verlag, Berlin.

Reimer, P.J., Bard, E., Bayliss, A., Beck, J.W., Blackwell, P.G., Bronk Ramsey, C., Buck, C.E., Cheng, H., Edwards, R.L., Friedrich, M., Grootes, P.M., Guilderson, T.P., Haflidason, H., Hajdas, I., Hatté, C., Heaton, T.J., Hoffmann, D.L., Hogg, A.G., Hughen, K.A., Kaiser, K.F., Kromer, B., Manning, S.W., Niu, M., Reimer, R.W., Richards, D.A., Scott, E.M., Southon, J.R., Staff, R.A., Turney, C.S.M., van der Plicht, J., 2013. IntCal13 and Marine13 Radiocarbon Age Calibration Curves 0–50,000 Years Cal BP.

Santos, G.M., Ormsby, K., 2013. Behavioral variability in ABA chemical pretreatment close to the 14C age limit. Radiocarbon 55 (2–3), 534–544.

Santos, G.M., Southon, J.R., Druffel-Rodriguez, K.C., Griffin, S., Mazon, M., 2004. Magnesium perchlorate as an alternative water trap in AMS graphite sample preparation: a report on sample preparation at KCCAMS at the University of California, Irvine. Radiocarbon 46 (1), 165–173.

Santos, G.M., Xu, X., 2016. Bag of tricks: a set of techniques and other resources to help 14C laboratory setup, sample processing, and beyond. Radiocarbon 1–17. FirstView.

Santos, G.M., M, R.B., Southon, J.R., Griffin, S., Hinger, E., Zhang, D., 2007. AMS 14C sample preparation at the KCCAMS/UCI facility: status report and performance of small samples. Radiocarbon 49 (2), 255–269.

Schneider, B., Hoffmann, G., Reicherter, K., 2016. Scenario-based tsunami risk assessment using a static flooding approach and high-resolution digital elevation data: an example from Muscat in Oman. Glob. Planet. Change 139, 183–194.

Sirocko, F., Sarnthein, M., Erlenkeuser, H., et al., 1993. Century scale events in monsoonal climate over the past 24,000 years. Nature 364, 322–324.

Southon, J., Kashgarian, M., Fontugne, M., Metivier, B., Yim, W.W.-S., 2002. Marine reservoir corrections for the Indian Ocean and Southeast Asia. Radiocarbon 44 (1), 167–180.

Staubwasser, M., Sirocko, F., Grootes, P.M., Erlenkeuser, H., 2002. South Asian monsoon climate change and radiocarbon in the Arabian Sea during early and middle Holocene. Paleoceanography 17 (4), 1063.

Staubwasser, M., Sirocko, F., Grootes, P.M., Segl, M., 2003. Climate change at the 4.2 ka BP termination of the Indus valley civilization and holocene south Asian monsoon variability. Geophys. Res. Lett. 30 (8), 15-1–15-2.

Steinhof, A., Adamiec, G., Gleixner, G., van Klinken, G.J., Wagner, T., 2004. The new 14C analysis laboratory in Jena, Germany. Radiocarbon 46 (1), 51–58.

Stuiver, M., Polach, H.A., 1977. Discussion: Reporting of 14C Data. Radiocarbon 19 (3), 355–363.

Uerpmann, H.-P., M. Uerpmann, M. Hinderer, S. Lindauer, C. Neureiter, R. Ghukasyan, S. Kesejyan and A. Petrosyan (under review). HLO1-South: an early neolithic site in the Wadi al-Hilo (Sharjah, UAE). Arab. Archaeol. Epigr.

Van Rampelbergh, M., Fleitmann, D., Verheyden, S., Cheng, H., Edwards, L., De Geest, P., De Vleeschouwer, D., Burns, S.J., Matter, A., Claeys, P., Keppens, E., 2013. Mid- to late Holocene Indian Ocean monsoon variability recorded in four speleothems from socotra Island, Yemen. Quat. Sci. Rev. 65, 129–142.

Wacker, L., Fülöp, R.H., Hajdas, I., Molnár, M., Rethemeyer, J., 2013. A novel approach to process carbonate samples for radiocarbon measurements with helium carrier gas. Nucl. Instrum. Meth. Phys. Res. Sect. B Beam Interact. Mater. Atoms 294 (0), 214–217.

Weninger, B., Clare, L., Rohling, E., Bar-Yosef, O., Boehner, U., Budja, M., Bundschuh, M., Feurdean, A., Gebe, H.G., Joeris, O., Lindstaedter, J., Mayewski, P., Muehlenbruch, T., Reingruber, A., Rollefson, G., Schyle, D., Thissen, L., Todorova, H., Zielhofer, C., 2009. The impact of rapid climate change on prehistoric societies during the Holocene in the Eastern Mediterranean. Doc. Praehist. 36, 7–59.

Zazzo, A., Munoz, O., Badel, E., Béguier, I., Genchi, F., Marcucci, L.G., 2016. A revised radiocarbon chronology of the Aceramic shell midden of Ra's Al-Hamra 6 (Muscat, Sultanate of Oman): Implication for occupational sequence, marine reservoir age, and human mobility. Radiocarbon 58 (2), 383–395.

Zazzo, A., Munoz, O., Saliège, J.F., Moreau, C., 2012. Variability in the marine radiocarbon reservoir effect in Muscat (Sultanate of Oman) during the 4th millennium BC: reflection of taphonomy or environment? J. Archaeol. Sci. 39 (7), 2559–2567.